Supplementary Figure 1

Supplementary Figure 1A-E: SPOP mRNA expression is frequently down-regulated in human prostate cancer. Box-and-whisker plots of SPOP mRNA expression levels in five different publicly available prostate cancer datasets (normal/benign, primary cancer and, where available, metastatic cancer). The findings in Panel B were previously reported in Barbieri et al. 2012 *Nature Genetics* study and are included here for comparison.

*p-value<0.001. Black asterisks indicate comparison of normal/benign group against primary and red asterisks indicate comparison of primary group with metastases or CRPC (as applicable).

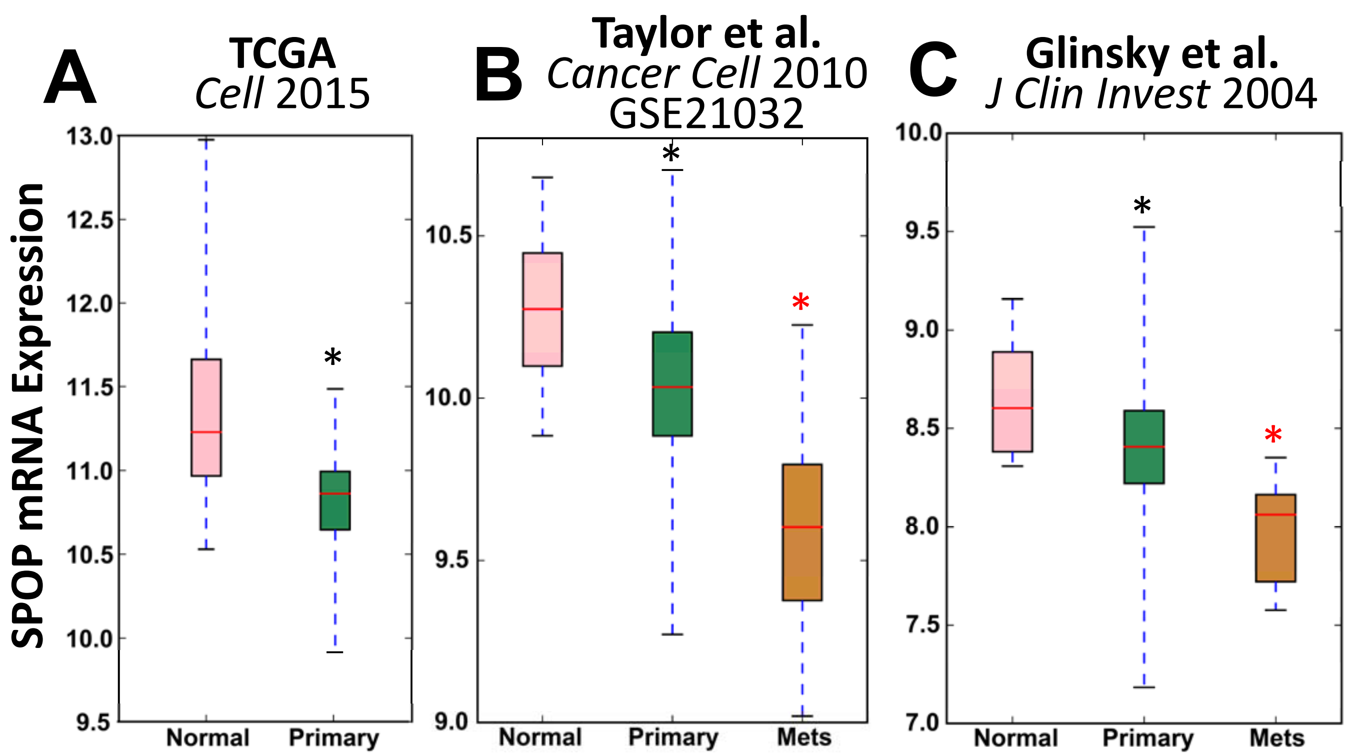

Supplementary Figure 1

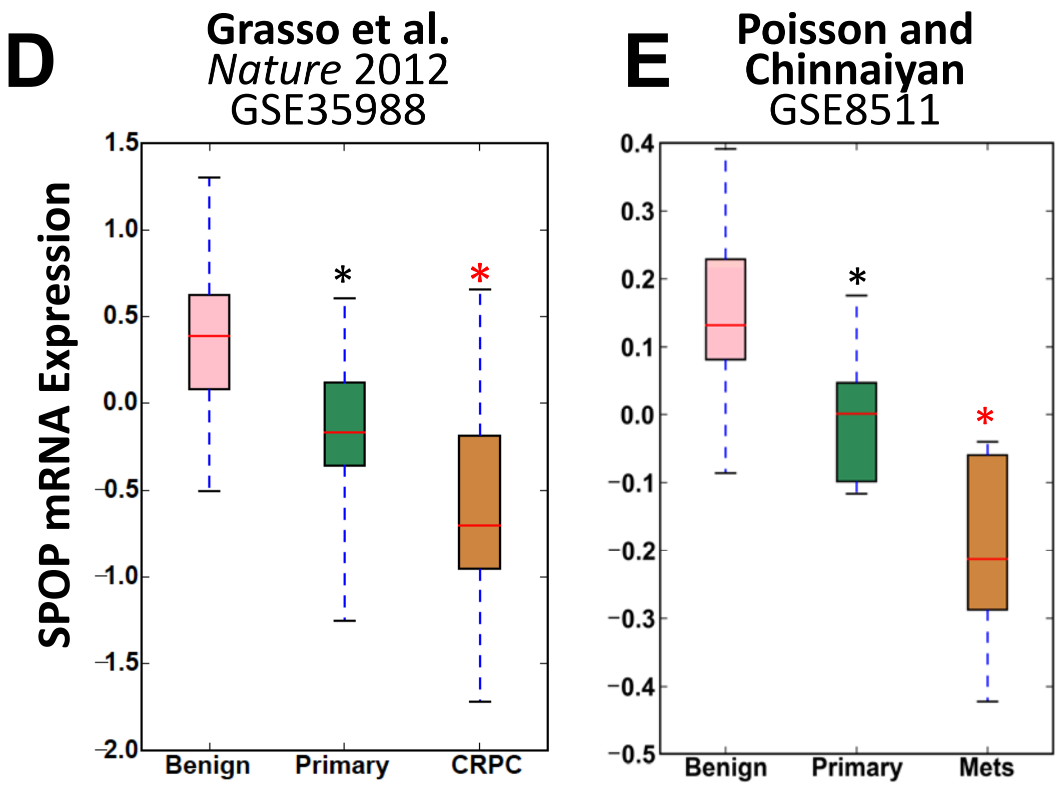

Supplementary Figure 2

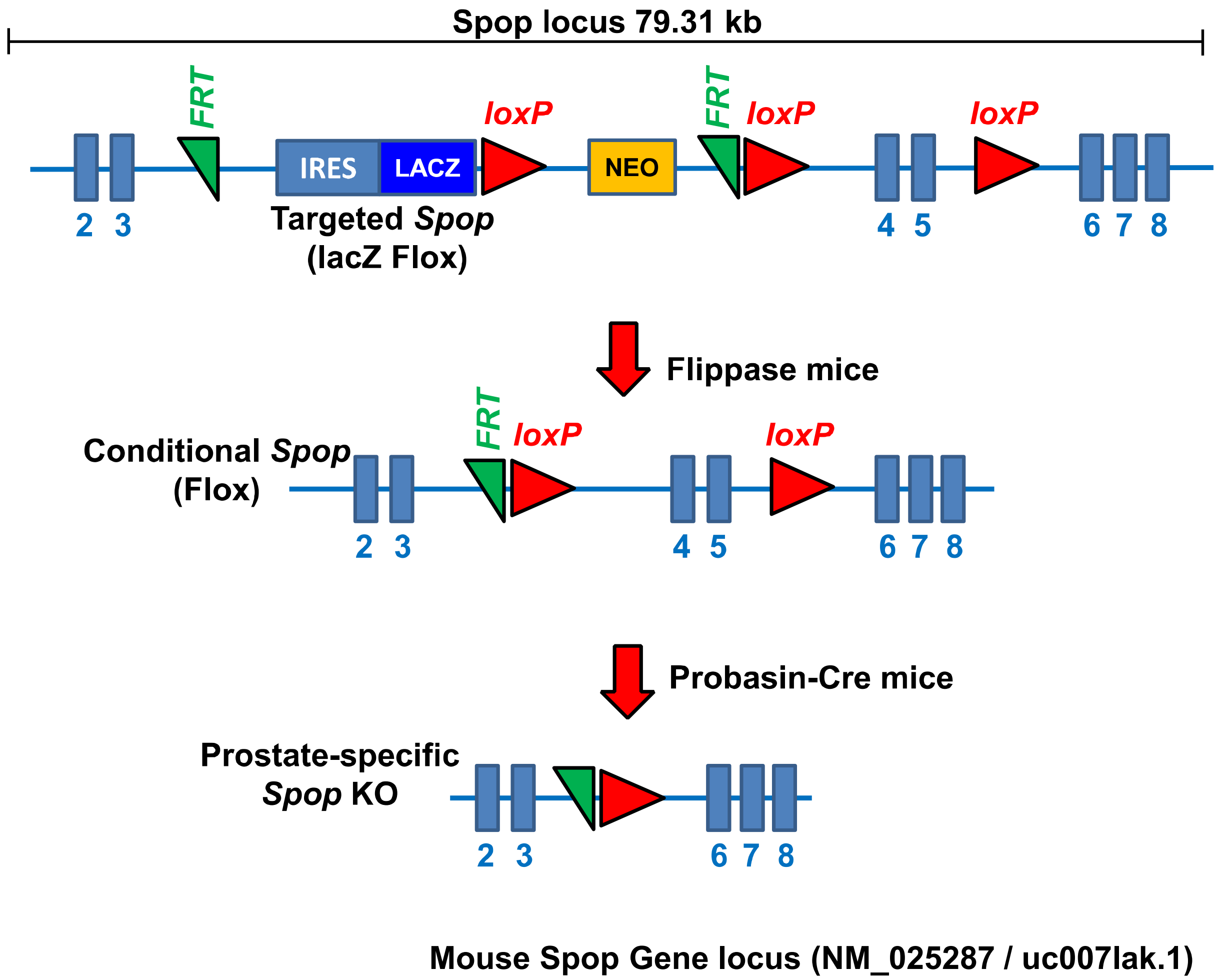

Supplementary Figure 2: Schematic representation of the *Spop* genomic locus in a whole-body heterozygous mouse model and a prostate-specific *Spop*-ablated mouse model. Schematic representation of the murine *Spop* genomic locus in *Spop* Knockout-First-Reporter Tagged Insertion mice (*Spop*^{tm1a}(KOMP)Wtsi), where a cassette containing β-galactosidase (LacZ) and neomycin-resistance genes was engineered into the *Spop* locus (after exon 3), interrupting the expression of the full-length Spop and resulting in a non-expressive allele. We then crossed the *Spop*$^{tm1a(KOMP)Wtsi}$ mice with ROSA-Flp mice (with the Flippase gene knocked into the ROSA26 locus), in order to remove the LacZ and neomycin-resistance cassettes and generate *Spop* floxed alleles (*Spop*^{fl}), where *Spop* exons 4 and 5 (encoding the core of the MATH domain) are flanked by loxP sites. Crossing with a probasin (PB)-Cre transgenic mouse line results in selective ablation of the *Spop* allele in the prostate luminal epithelium.

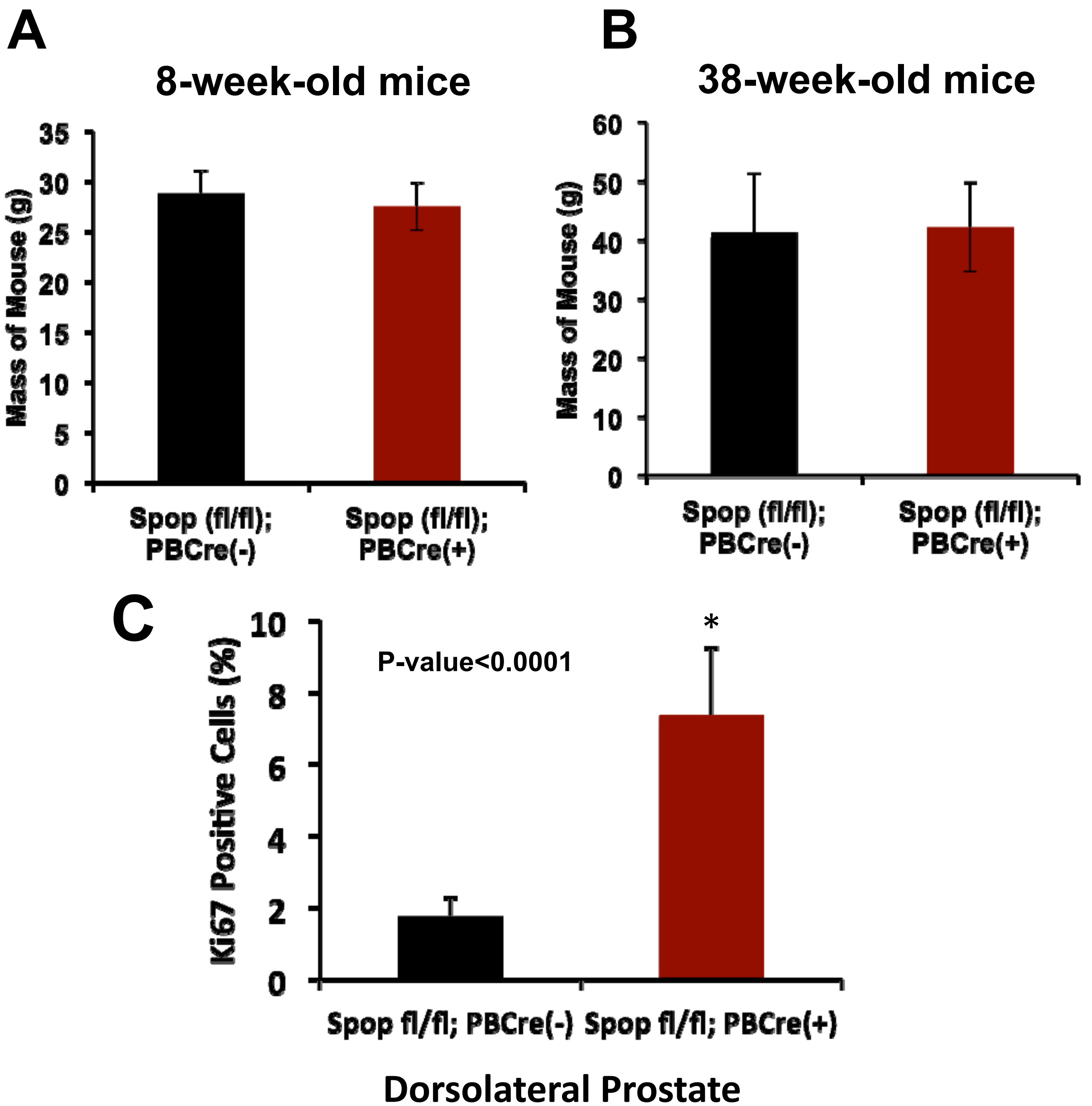

Supplementary Figure 3: Overall body mass of mice with biallelic prostate-specific deletion of *Spop*. A. Overall body mass of $Spop^{fl/fl}$;*PBCre(-)* (n=13) and $Spop^{fl/fl}$;*PBCre(+)* (n=10) mice (measured at 8 weeks of age) . **B**. Overall body mass of $Spop^{fl/fl}$;*PBCre(-)* and $Spop^{fl/fl}$;*PBCre(+)* mice (measured at 38 weeks of age). **C.** Quantification of Ki67 staining in the dorsolateral prostate lobes of 8-week-old $Spop^{fl/fl}$;*PBCre(-)* (n=7) and $Spop^{fl/fl}$;*PBCre(+)* (n=8) mice. Mean with SD is shown.

Supplementary Figure 4

Supplementary Figure 4: Prostate-specific biallelic ablation of *Spop* leads to elevated expression of AR and c-MYC proteins. A-B. Higher magnification of c-MYC IHC of ventral and dorsolateral prostate of 8-week-old *Spop*$^{fl/fl}$;*PBCre(-)* and *Spop*$^{fl/fl}$;*PBCre(+)* mice. Prostate sections from 7 *Spop*$^{fl/fl}$;*PBCre(-)* and 8 *Spop*$^{fl/fl}$;*PBCre(+)* mice were stained with c-MYC. Four representative images are shown. **C-D.** Quantification of the protein expression changes noted in the immunoblot analyses for AR and c-MYC in the 8-week-old *Spop*$^{fl/fl}$;*PBCre(-)* and *Spop*$^{fl/fl}$;*PBCre(+)* mice.

A

***Spop* (fl/fl); PBCre(-)**

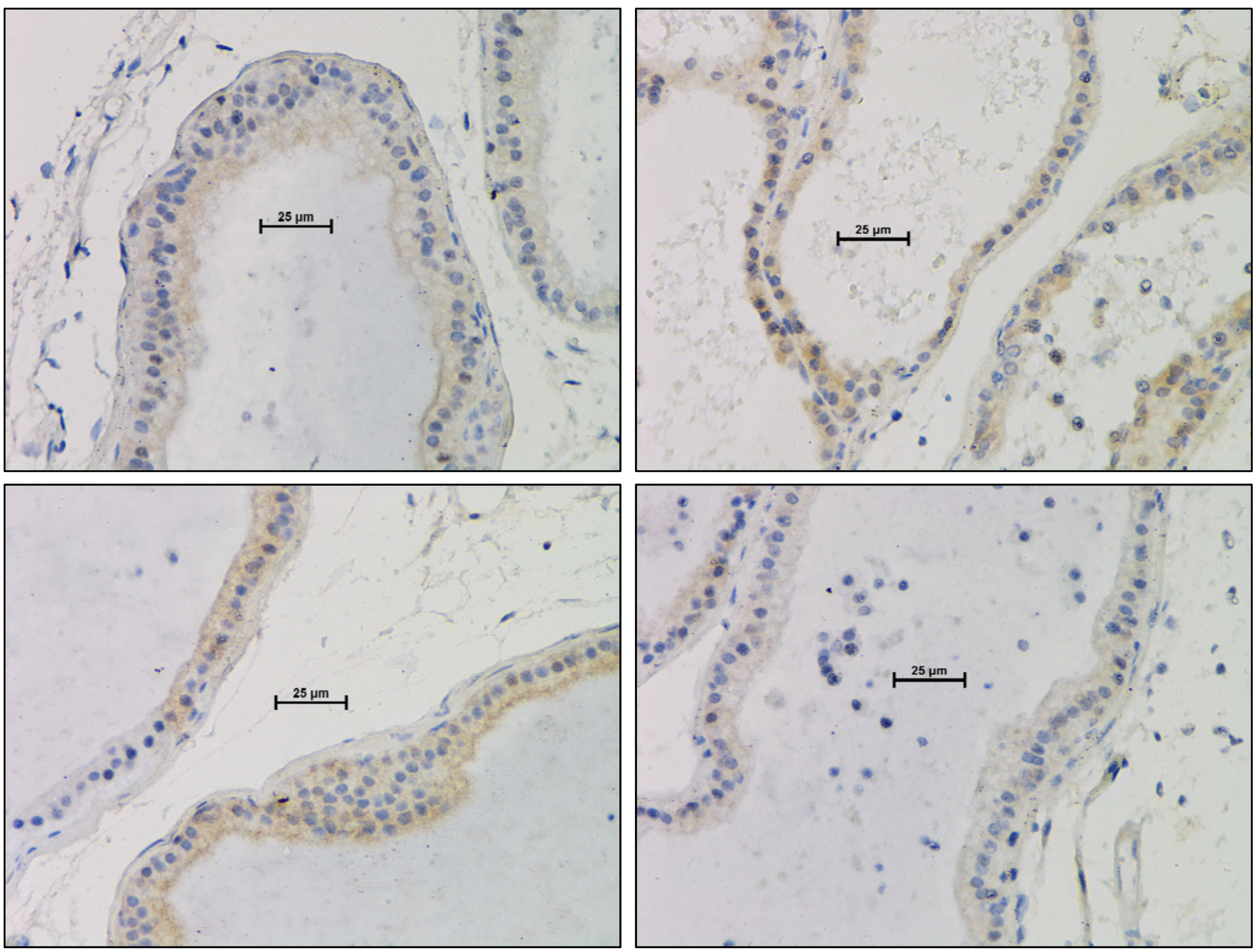

c-MYC

B

***Spop* (fl/fl); PBCre(+)**

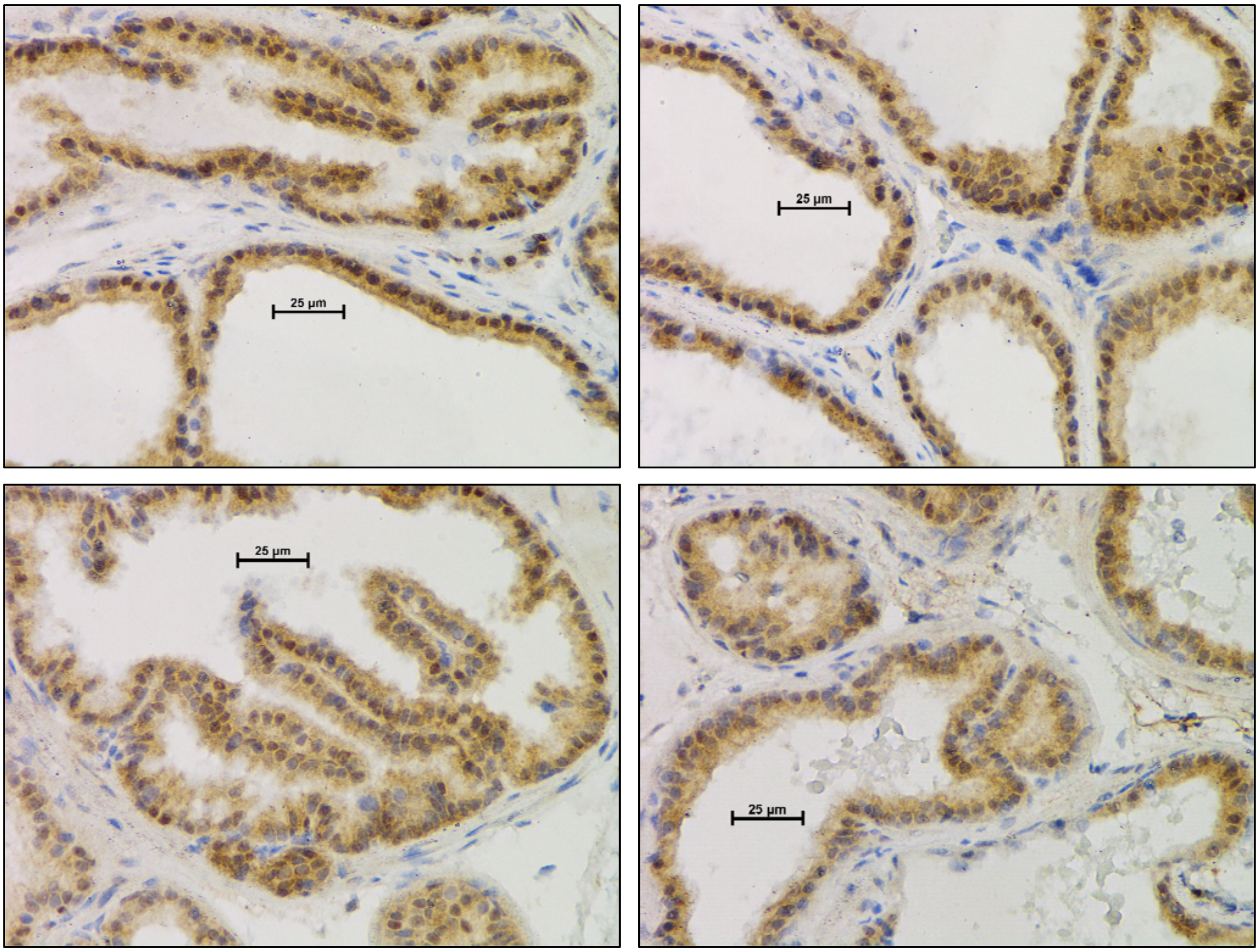

c-MYC

Supplementary Figure 4